Technobius Physics, 2025, 3(1), 0028, DOI: https://doi.org/10.54355/tbusphys/3.1.2025.0028

Technobius Physics

https://technobiusphysics.kz/

e-ISSN 3007-0147

Article

Experimental determination of X-ray absorption and K-edge behavior in metal foils

Sanzhar Serik*

Department of Physics, School of Science and Humanities, Nazarbayev University, Astana, Kazakhstan
*Correspondence: sanzhar.serik.00@bk.ru

Abstract. This study investigates the absorption behavior of X-rays in various metallic foils, focusing on the dependence of transmitted intensity and mass attenuation coefficient (μ/ρ)s on material thickness and radiation wavelength. The objective was to experimentally validate theoretical models of X-ray attenuation and to determine the position of K absorption edges for selected elements. Using a goniometer-based X-ray setup equipped with a Geiger-Müller counter, a series of measurements were conducted on aluminum, zinc, tin, copper, and nickel foils under controlled conditions. The first part of the experiment demonstrated an exponential decrease in transmitted intensity with increasing absorber thickness. The second part established a cubic dependence of the mass attenuation coefficient (μ/ρ)on the wavelength of the incident X-rays, consistent with theoretical expectations for photoelectric absorption. In the third part, distinct K absorption edges were successfully identified for copper and nickel, with experimentally determined edge energies closely matching known values. The results confirmed that materials with higher atomic numbers exhibit greater absorption and sharper K-edges. Minor deviations observed near absorption thresholds were attributed to spectral interference and detector resolution limitations. Overall, the study validated key theoretical relationships and demonstrated the effectiveness of the experimental setup for accurately characterizing X-ray absorption behavior in metals.
Keywords: X-ray absorption, mass attenuation, K-edge detection, metal foils, wavelength dependence.

1. Introduction

X-ray absorption is a fundamental interaction between high-energy photons and matter, characterized by a reduction in intensity as X-rays pass through different media. This phenomenon underpins numerous applications, including non-destructive testing, medical diagnostics, and elemental analysis. A key parameter in quantifying this interaction is the mass attenuation coefficient $\sqrt[3]{\mu/p}$, which depends on the atomic number Z, density, and photon energy or wavelength of the incident radiation. The primary mechanism governing absorption in this context is the photoelectric effect, particularly dominant at lower photon energies and in materials with higher atomic numbers.

Accurate determination of $\sqrt[3]{\mu/p}$ is essential for practical applications involving shielding design, spectroscopic material analysis, and imaging systems calibration. Although theoretical models predict an inverse cubic relationship with photon energy, experimental validation remains critical, especially near sharp absorption edges such as the K-edge, where the incident photon energy becomes sufficient to eject core electrons.

Recent studies have refined the experimental measurement of mass attenuation coefficients. The authors developed a versatile laboratory X-ray absorption spectrometer capable of multi-mode detection and demonstrated accurate edge resolution for several metals [1]. In another study, authors provided experimentally measured attenuation coefficients for elements ranging from low to medium atomic numbers, identifying deviations in regions close to absorption edges [2]. Scientists investigated energy-dependent attenuation in various alloys and confirmed that deviations from

theoretical predictions occur due to structural variations in crystalline materials [3]. Furthermore, researchers presented comprehensive data for transition metals, validating the dependence of $\sqrt[3]{\mu/p}$ on λ^3 and identifying systematic differences near absorption thresholds [4]. These investigations collectively highlight both progress and remaining limitations in achieving high precision near abrupt energy transitions.

Despite these advances, existing studies often focus on isolated materials or energy ranges, limiting the ability to generalize results across a broad set of metals under unified experimental conditions. Moreover, practical constraints such as spectral overlap, detector resolution, and second-order interference continue to affect the accuracy of K-edge determination.

To address this gap, we hypothesize that by employing a calibrated goniometer-based experimental chamber with a Geiger-Müller (GM) detector, it is possible to experimentally verify theoretical models of X-ray attenuation and accurately determine the mass attenuation coefficients and K-edge energies for a range of metals. Specifically, we anticipate confirming the exponential attenuation of X-ray intensity with absorber thickness, the cubic dependence of $\sqrt[3]{\mu/p}$ on wavelength, and the identification of element-specific K-edges.

The objective of this study is to experimentally determine the mass attenuation coefficient $\sqrt[3]{\mu/p}$ for aluminum, zinc, tin, copper, and nickel as functions of both material thickness and incident X-ray wavelength. This work combines three structured experimental tasks into a unified investigation, aiming to validate key theoretical relationships and improve the reliability of educational and practical X-ray absorption measurements. The novelty lies in its comprehensive, comparative approach using a consistent apparatus setup across all materials.

2. Methods

X-ray absorption experiments were conducted using a standard goniometer-based experimental chamber equipped with an analyser crystal and a GM counter tube. The goniometer (by Leybold Company P2540105) was connected to the X-ray unit and the counter tube via dedicated sockets. The analyser crystal was mounted at the terminal position on the right-hand rail, and the GM counter was fixed to the back stop using a standard holder. A diaphragm was placed in front of the GM tube to limit background radiation, while a 2 mm diaphragm tube was inserted into the beam outlet of the X-ray tube plug-in unit. The X-ray system was connected to a computer via USB for data acquisition and control.

For absorption of X-rays as a function of material thickness foils of aluminium and tin with varying thicknesses were inserted manually into the diaphragm in front of the GM counter. Two characteristic glancing angles were selected to represent both characteristic line emission and bremsstrahlung regions: 20.4° for the copper Kβ line and ~10° for bremsstrahlung. For each selected angle, the intensity was recorded without absorber (I_0) and with the foil absorber (I), using a gate timer with an integration time of 50 s. To improve statistical reliability and minimize relative errors, measurements were conducted until the pulse rate was below 1000 counts per second. Data were collected for single foils and for paired foils to simulate increased absorber thickness.

For determination of the mass absorption coefficient as a function of wavelength absorption spectra were recorded using aluminium (d = 0.08 mm) and tin (d = 0.025 mm) foils separately. For each material, glancing angles were scanned in the range of 6° to 16° with steps of 1–2°, while maintaining a minimum integration time of 50 s. A reference spectrum (I_0) without any absorber was also recorded under identical conditions. Using Bragg's law, the glancing angles were converted to corresponding wavelengths (λ), and the mass absorption coefficients (μ/ρ) were calculated by evaluating the transmission ratio I/I_0 and applying the Beer–Lambert law [5].

For determination of the absorption coefficient for copper and nickel a similar procedure was followed using copper and nickel foils (d = 0.025 mm), with spectra recorded over a wider angular range of 6°–25°, using 1° steps. In regions near the absorption edges, finer angular steps (<1°) were applied to accurately capture rapid changes in absorption. While the default anode voltage was 35

kV, improved spectral resolution was achieved at 20–25 kV by increasing integration times accordingly. The resulting data were used to plot absorption coefficients as a function of the wavelength of primary radiation.

All measurements were conducted under stable environmental conditions, and each dataset was statistically analysed using OriginPro 2021 software. The coefficient of variation was computed to assess the reproducibility of intensity measurements.

3. Results and Discussion

Figure 1 presents the measured ratio of transmitted to initial intensity ($\frac{I}{I_0}$) as a function of absorber thickness *d* for aluminium and zinc foils of varying thicknesses.

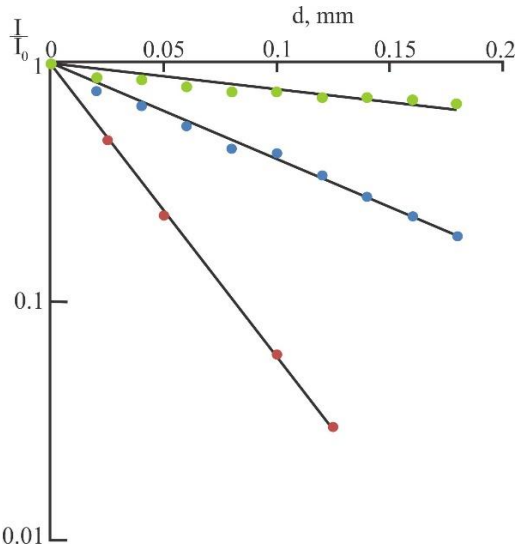

Figure 1 – Semi-logarithmic representation of the quotient as a function of the absorber thickness d

In Figure 1, three distinct exponential decay curves are observed. Curves 1 and 2 correspond to aluminium (Z = 13, ρ = 2.70 g/cm³), while curve 3 corresponds to zinc (Z = 30, ρ = 7.14 g/cm³). As the absorber thickness increases, the relative transmitted intensity $\frac{I}{I_0}$ decreases exponentially, consistent with the Beer–Lambert law [5]. The attenuation is significantly stronger for zinc than for aluminium, confirming the well-known dependence of X-ray absorption on atomic number Z.

Comparing curves 1 and 3 at the same primary radiation energy, zinc demonstrates a markedly higher absorption capacity. Additionally, comparing curves 1 and 2 for aluminium under different glancing angles (i.e., different radiation energies), a decrease in absorption is noted at higher photon energies. These observations are in agreement with theoretical predictions, where absorption is directly related to Z and inversely to photon energy. The complete dataset derived from these measurements is provided in Table 1.

Table 1 – Dependence of the absorption on the wavelength

Al (Z = 13)	μ, cm^{-1}	$d_{1/2}$, cm	$\frac{\mu}{\rho}$, $cm^2 g^{-1}$
ρ = 2.7 g/cm^3			
λ = 139 pm	112	$6.2 \cdot 10^{-3}$	41.5
λ = 70 pm	14.1	20.4	5.2
Zn (Z = 30)			
ρ = 7.14 g/cm^{-3}			
λ = 139 pm	280	$2.5 \cdot 10^{-3}$	39.2

These results reinforce the understanding that higher-Z materials more effectively attenuate X-rays and that attenuation diminishes with increasing photon energy. However, as the primary radiation energy lies within the K-edge of zinc, the simplified Z-dependence of the mass absorption coefficient is not fully applicable in this region.

Figure 2 illustrates the cubic root of the mass absorption coefficient $(\mu/\rho)^3$ as a function of the X-ray wavelength (λ) for aluminium and tin foils, each with a fixed thickness.

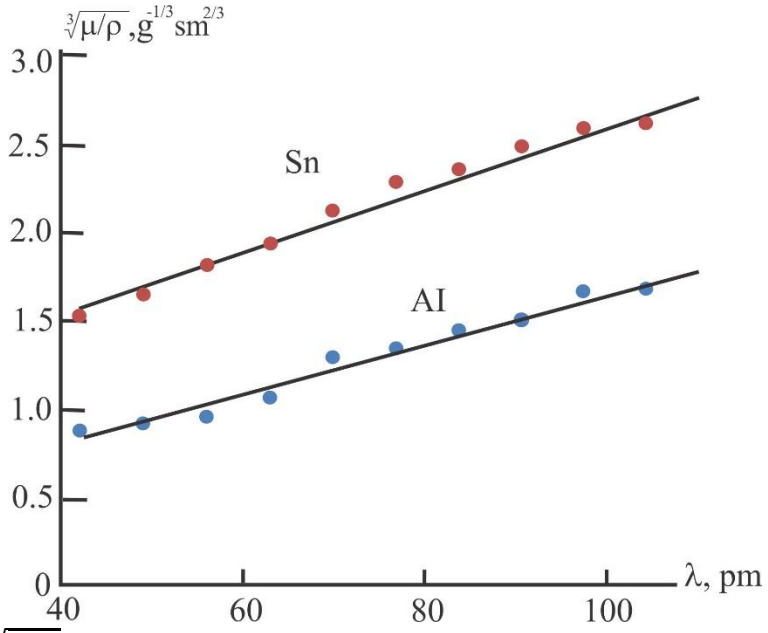

Figure 2 – $\sqrt[3]{\mu/p}$ for aluminium and tin as a function of the primary radiation energy

After converting glancing angles to wavelengths using Bragg's law [5], the experimental data were processed to determine $\sqrt[3]{\mu/p}$ for each material. The plotted values of $\sqrt[3]{\mu/p}$ against λ demonstrate a clear linear trend for both aluminium and tin, confirming the theoretical dependence with a higher atomic number (Z = 50, ρ = 7.28 g/cm³), consistently exhibits greater absorption values compared to aluminium, as reflected by the higher position of its trend line. These linear dependencies validate the suitability of the Beer–Lambert model and confirm that the dominant absorption mechanism in this range is photoelectric in nature, where the absorption cross-section increases steeply with decreasing photon energy and increasing atomic number. The trends observed in both experiments strongly support classical X-ray absorption theory. The exponential decrease of transmitted intensity with thickness (Figure 1) aligns with expectations from fundamental attenuation laws, while the wavelength-dependence of μ/ρ (Figure 2) is consistent with the known power-law behavior for photoelectric absorption. The strong dependence on Z is also clearly visible when comparing aluminium, tin, and zinc. These findings are consistent with prior experimental studies [6], [7], confirming the reliability of the experimental setup and procedure.

Minor deviations from ideal exponential behavior at certain wavelengths may be attributed to proximity to absorption edges or instrumental limitations, including GM tube response time or diaphragm alignment. For future experiments, finer step sizes near K-edges and higher-resolution detectors could improve precision.

Figures 3 and 4 show the cubic root of the mass absorption coefficient $\sqrt[3]{\mu/p}$ as a function of the X-ray wavelength λ for copper and nickel foils, respectively.

In both graphs, a linear correlation between $\sqrt[3]{\mu/p}$ and λ is evident in the region where $\lambda \neq \lambda_K$. However, near the so-called *K* absorption edge ($\lambda = \lambda_K$), a distinct discontinuity occurs. This jump corresponds to the photon energy surpassing the binding energy of the K-shell electrons, enabling photoionization. For copper (Z = 29, ρ = 8.96 g/cm³), this edge appears at λ_K = 138 pm, while for nickel (Z = 28, ρ = 8.99 g/cm³), the edge is at λ_K = 149 pm.

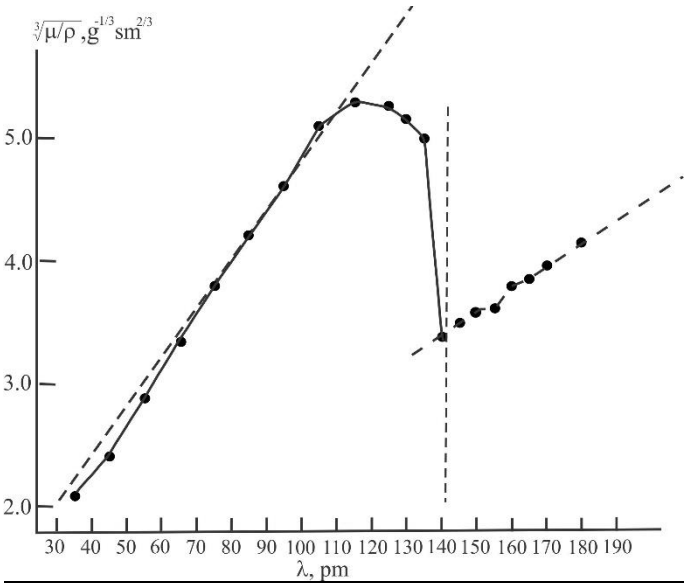

Figure 3 – Absorption edge of Cu: U_A =25 kV, λ_K =138 pm

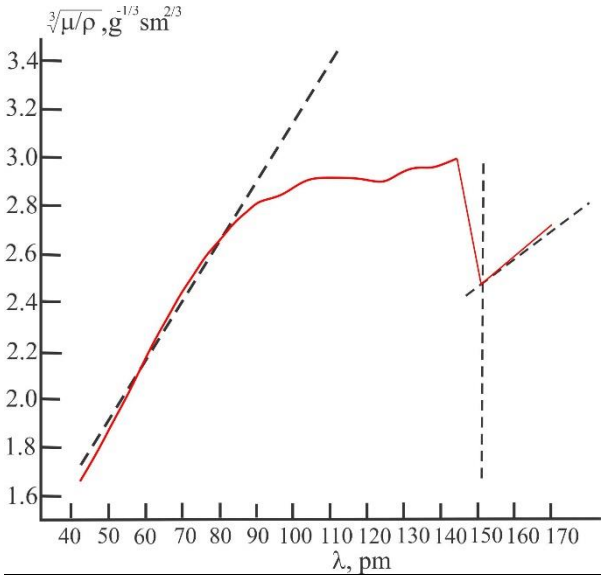

Figure 4 – Absorption edge of Ni: U_A =25 kV, λ_K =149 pm

Below these thresholds (λ < 70 pm), both curves deviate from linearity due to increased intensity of the primary radiation from second-order diffraction or interference effects. According to the Bragg condition for cooper λ_K=138 pm → E_K = 8.98 keV and for nickel λ_K=149 pm → E_K = 8.32 keV. These values confirm the accuracy of the experiment. Since $Z_{Ni} < Z_{Cu}$, the absorption edge for nickel occurs at a longer wavelength and lower energy than for copper, as expected.

The trends in Figures 3 and 4 are consistent with classical X-ray absorption theory. A linear relationship between $\sqrt[3]{\mu/p}$ and λ is valid outside the absorption edge, confirming the proportionality $\mu/\rho \propto \lambda^3$. A sharp increase in absorption at $\lambda = \lambda_K$ is a characteristic feature of K-edge transitions. The difference in λ_K between copper and nickel correlates with their atomic numbers, validating the theoretical expectation that higher-Z elements have lower λ_K and higher K-shell binding energies. These results confirm that the mass absorption coefficient is strongly dependent on both wavelength and atomic structure. The deviation from linearity at shorter wavelengths is attributed to higher-order harmonics in the bremsstrahlung spectrum, which lead to overestimated transparency of the absorber.

4. Conclusions

The study successfully investigated the absorption behavior of X-rays as a function of material thickness and wavelength for aluminium, tin, copper, and nickel foils using GM detection and goniometer-based measurements. An exponential decrease in transmitted intensity $\frac{I}{I_0}$ with increasing absorber thickness was observed, confirming the Beer–Lambert law. Zinc exhibited significantly higher absorption than aluminium at equal thicknesses due to its higher atomic number (Z = 30; Z = 13). A linear relationship between $\sqrt[3]{\mu/p}$ and wavelength λ was confirmed for aluminium and tin, supporting the empirical law $\mu/\rho \propto \lambda^3$. Tin showed greater absorption than aluminium due to its higher Z (Z = 50; Z = 13). Distinct K absorption edges were identified for copper (λ_K=138 pm → E_K = 8.98 keV) and nickel (λ_K=149 pm → E_K = 8.32 keV), in agreement with theoretical expectations based on atomic number.

The study addressed the research objective by demonstrating the dependence of X-ray absorption on both absorber thickness and primary radiation wavelength, and by quantitatively determining the absorption edge energies. The results may be used in educational settings to demonstrate X-ray absorption principles or in material identification based on spectral edge analysis. Limitations include spectral resolution near absorption edges and second-order interferences at short

wavelengths. Further studies may involve higher-resolution detectors and more precise step sizes around λ_K to improve accuracy.

References

[1] G. Bunker, "X-ray absorption spectrometers," *Encycl. Spectrosc. Spectrom.*, pp. 610–616, Jan. 2016, doi: 10.1016/B978-0-12-409547-2.05066-6.
[2] R. Hauko, J. P. Gomilšek, I. Arčon, and A. Kodre, "Absolute determination of the x-ray absorption coefficient of strontium in the K edge region," *Radiat. Phys. Chem.*, vol. 103, pp. 203–208, 2014, doi: 10.1016/J.RADPHYSCHEM.2014.05.059.
[3] O. Paul, S. Toscano, K. Totland, and M. Landolt, "The spatial origin of the spin-polarization of secondary-electron emission from Fe," *Surf. Sci.*, vol. 251–252, no. C, pp. 27–30, Jul. 1991, doi: 10.1016/0039-6028(91)90947-Q.
[4] M. T. Murphy and J. C. Berengut, "Laboratory atomic transition data for precise optical quasar absorption spectroscopy," *Mon. Not. R. Astron. Soc.*, vol. 438, no. 1, pp. 388–411, 2014, doi: 10.1093/MNRAS/STT2204.
[5] L. Li *et al.*, "Study on the origin of linear deviation with the Beer-Lambert law in absorption spectroscopy by measuring sulfur dioxide," *Spectrochim. Acta - Part A Mol. Biomol. Spectrosc.*, vol. 275, Jul. 2022, doi: 10.1016/J.SAA.2022.121192.
[6] Y. Sun, R. Hong, C. Tao, and D. Zhang, "Design and Optical Field Tuning of ITO Multi-Layer Films Based on Tamm Plasmon Effect," *Zhongguo Jiguang/Chinese J. Lasers*, vol. 51, no. 22, Nov. 2024, doi: 10.3788/CJL240479.
[7] W. Lu *et al.*, "Recent progress of multilayer composite transparent conductive film," *Kexue Tongbao/Chinese Sci. Bull.*, vol. 62, no. 5, pp. 372–384, Feb. 2017, doi: 10.1360/N972016-01133.

Information about authors:
Sanzhar Serik – MS, Research assistant, Department of Physics, School of Science and Humanities, Nazarbayev University, Astana, Kazakhstan, sanzhar.serik.00@bk.ru

Author Contributions:
Sanzhar Serik – concept, methodology, resources, data collection, testing, modeling, analysis, visualization, interpretation, drafting, editing, funding acquisition.

Conflict of Interest: The authors declare no conflict of interest.

Use of Artificial Intelligence (AI): The authors declare that AI was not used.

Received: 15.02.2025
Revised: 24.02.2025
Accepted: 25.03.2025
Published: 29.03.2025